Purpurogallin carboxylic acid exhibits synergistic effects with 5-fluorouracil on liver cancer cells *in vitro* by targeting ABCG2

PINGPING ZHAO[1*], WEI LIU[1*], SHUQING WANG[2] and JUNJIE LUN[1]

[1]Department of Oncology, Changle County People's Hospital Affiliated to Weifang Medical College, Weifang, Shandong 261000, P.R. China; [2]Department of Traditional Chinese Medicine, Affiliated Hospital of Weifang Medical College, Weifang, Shandong 261000, P.R. China

Received June 2, 2023; Accepted April 22, 2024

DOI: 10.3892/etm.2024.12564

Abstract. Purpurogallin carboxylic acid (PCA) is a natural phenol compound derived from *Macleaya microcarpa* (Maxim.) Fedde, which exerts particular antioxidant and anti-inflammatory capacities. However, the effects and mechanisms of PCA on liver cancer cells remain unknown. Therefore, network pharmacology and computer virtual docking were used to identify the target-proteins of PCA. In addition, surface plasmon resonance, protease activity and rhodamine excretion assays were carried out to evaluate the effects of PCA on the activity of ATP binding cassette subfamily G member 2 (ABCG2). The synergistic effects of PCA and 5-fluorouracil (5-FU) on liver cancer cell proliferation, cell cycle arrest, colony formation and spheroid formation abilities *in vitro* were determined by Cell Counting Kit-8 (CCK-8) assay, flow cytometry, western blot analysis, colony formation and spheroid formation assays, respectively. ABCG2 was identified as a potential target of PCA, with a high docking score. The equilibrium dissociation constant of PCA for ABCG2 protein was 1.84 μM, while the median inhibitory concentration of this protein was 3.09 μM. In addition, the results demonstrated that PCA could significantly reduce the drug efflux capacity of liver cancer cells. CCK-8 assays revealed that liver cancer cell treatment with 10 μM PCA and 10 μM 5-FU exhibited the most potent synergistic effects on liver cancer cell proliferation at 48 h. Additionally, cell co-treatment with PCA and 5-FU also significantly attenuated the colony and spheroid formation abilities of liver cancer cells *in vitro,* while it promoted their arrest at the G_1 phase of the cell cycle. Furthermore, ABCG2 silencing in liver cancer cells notably abrogated the synergistic effects of PCA and 5-FU. In conclusion, the present study demonstrated that PCA exhibited synergistic effects with 5-FU on liver cancer cells *in vitro* via targeting ABCG2. Therefore, PCA combined with 5-FU may be a potential strategy for liver cancer therapy.

Correspondence to: Professor Junjie Lun, Department of Oncology, Changle County People's Hospital Affiliated to Weifang Medical College, 278 Limin Road, Weifang, Shandong 261000, P.R. China
E-mail: lunjunjie001@163.com

*Contributed equally

Key words: liver cancer, purpurogallin carboxylic acid, synergistic effect, 5-fluorouracil, ATP binding cassette subfamily G member 2

Introduction

Liver cancer, a malignancy of the digestive system, accounts for <2 million deaths in China (1). Due to the lack of symptoms, patients with liver cancer are commonly diagnosed at an advanced stage of the disease, making them contraindicated for curative surgical therapy (2). Chemotherapy is the primary treatment approach for patients with advanced liver cancer, while 5-fluorouracil (5-FU) is one of the first-line chemotherapy drugs (3). However, due to its inherent toxicity to normal cells and multidrug resistance, 5-FU has limited clinical application (4). Currently, several natural products, such as curcumin (5) and quercetin (6), have been identified to exert synergistic effects with 5-FU, thus enhancing its efficacy. Consequently, novel chemosensitizers are urgently needed to treat patients with liver cancer.

Purpurogallin carboxylic acid (PCA; molecular formula, C12H8O7; IUPAC name, 2,3,4,6-tetrahydroxy-5-oxobenzo[7] annulene-8-carboxylic acid) is a natural phenol compound derived from *Macleaya microcarpa* (Maxim.) Fedde, which is also the oxidation product of gallic acid in fermented tea (7). Zeng *et al* (8) demonstrated that treatment with PCA could relieve corneal endothelial cell injury by reducing oxidative stress. Furthermore, Rambabu *et al* (9) revealed that PCA exhibited significant suppressive effects on the proliferation ability of MCF7 and A549 cancer cells by targeting claudin-4. However, its effects and molecular mechanisms on liver cancer cells remain elusive.

P-glycoproteins are promising drug efflux pumps, that have been extensively studied for their association with resistance to chemotherapeutic drugs (10,11). ATP binding cassette subfamily G member 2 (ABCG2) is a member of the P-glycoprotein family, which is upregulated in several types of cancer, including liver cancer (12). A previous study indicated that ABCG2 upregulation was associated with poor outcome in patients with liver cancer (13). Additionally, pharmacology- and genetic engineering technology-mediated ABCG2 downregulation could increase the sensitivity of liver cancer

cells to 5-FU (14). Therefore, exploring novel molecules to inhibit ABCG2 is a potential strategy for treating liver cancer.

The present study aimed to uncover the effects and underlying molecular mechanism of PCA on the behavior of liver cancer cells, thus suggesting that PCA could exert synergistic effects with 5-FU on liver cancer cells *in vitro* via targeting ABCG2.

Materials and methods

Network pharmacological analysis. The secondary structure of PCA was downloaded from PubChem Compound (https://www.ncbi.nlm.nih.gov/pccompound; accession no. 137628491). Subsequently, the secondary structure of PCA was imported into TargetNet (http://targetnet.scbdd.com/calcnet/index/) and Super-PERD (https://prediction.charite.de/) to predict the potential targets of PCA, with a possibility of ≥0.8. The predicted targets of PCA were visualized using Cytoscape (version 3.9.1; The Cytoscape Consortium). Finally, the intersected targets were used for further analysis.

Computer virtual docking. The crystal structure of ABCG2 (accession no. 6VXI), G protein-coupled receptor 35 (GPR35; accession no. 8H8J) and thyroid stimulating hormone receptor (TSHR; accession no. 4QT5) were downloaded from Protein Data Bank (https://www.rcsb.org/). Subsequently, the crystal structure of the aforementioned proteins was imported into SYBYL-X software (version 2.0; Tripos, Inc.; Certara) to perform structural optimization, including deletion of primary ligands, hydrogenation and adhesive end repair. Finally, the aforementioned proteins and the secondary structure of PCA were imported into AutoDock software (v1.5.6; UCSF Computer Graphics Laboratory) to perform flexible docking. Among them, ML230, a recognized ABCG2 inhibitor, was used as a positive control to compare the score of the binding between PCA and ABCG2. The binding sites between PCA and ABCG2 were visualized using PYMOL software (version 2.5; Schrödinger).

Surface plasmon resonance (SPR). Purified ABCG2 proteins were obtained from Sino Biological Inc. and were then desalinated using the AKTA protein purification system (Cytiva). Subsequently, proteins were dissolved in buffer solution (200 mM HEPES, 2 mM NaCl and 0.5% DMSO) and were conjugated with sodium acetate solution (pH 4.0) using the Biacore T200 system (Cytiva). Following conjugation with human metal-organic framework, an ethanolamine solution (1.0 M; Shanghai Ruji Biological Technology, Co., Ltd.) was used to block the uncoupled proteins at 28˚C for 6 h. The chip was then added to a buffer solution for 10 h. PCA was dissolved in the buffer solution (10 mmol/l HEPES, 150 mmol/l NaCl and 3 mmol/l EDTA) of the mobile phase. The binding constants between ABCG2 proteins and PCA were determined using a multi-cycle model. The flow rate of the mobile phase, the binding time and the dissociation time were set at 30 μl/sec, 240 and 300 sec, respectively.

Enzymatic activity determination. Firstly, all molecular reagents were dissolved in 1X Assay Buffer (5 mM $MgCl_2$, 50 μM $NADP^+$, NaCl 150 mM, pH 8.0 Tris-HCl 50 mM). Additionally, the purified ABCG2 proteins were diluted in a final concentration of 25 nM. Subsequently, a total of 35 μl/well protein dilution was added into a 384-well plate. Each well was then supplemented with 10 μl PCA reagent (0.01-100 μM) and incubated at room temperature for 1 h in the dark. Finally, the enzymatic reaction was initiated following the addition of 5 μl ATP/well. Following incubation for 30 min, the fluorescence intensity values were measured at a wavelength of 450 nm using the Varioskan LUX multifunctional microplate reader (Thermo Fisher Scientific, Inc.).

Cell culture and cell transfection with short interfering (si)RNA. The normal hepatocyte cell line, THLE-2, and the HepG2, Huh7 and Huh1 liver cancer cell lines were obtained from Procell Life Science & Technology Co., Ltd. All cell lines were authenticated by short tandem repeat (STR) DNA profiling analysis. THLE-2 cells were cultured in the corresponding special medium (https://www.procell.com.cn/view/10030.html; Procell Life Science & Technology Co., Ltd.) supplemented with 10% FBS, while HepG2, Huh7 and Huh1 cells were cultured in DMEM with 10% FBS (both from Hyclone; Cytiva). All cell lines were incubated at 37˚C in an incubator with 5% CO_2. The siRNAs targeting ABCG2 (si-ABCG2; sense, 5'-CUGGAGAUGUUCUGAUAAA-3' and antisense, 5'-UUUAUCAGAACAUCUCCAG-3') and the normal control siRNAs (si-NC; sense, 5'-UUCUCCGAACGUGUCACGU-3' and antisense, 5'-ACGUGACACGUUCGGAGAA-3') were purchased from GenePharma Co., Ltd. Cells were transfected with the aforementioned siRNAs (both 40 pmol) using Lipofectamine 2000® (Sangon Biotech Co., Ltd.), according to the manufacturer's instructions at 37˚C for 24 h. After 48 h, cells were used for performing biological experiments.

Rhodamine efflux assay. HepG2, Huh7 and Huh1 cells were seeded into a 6-well plate at a density of $1x10^5$ cells/well. Subsequently, adhered cells were treated with various concentrations of PCA (0, 2.5, 5 and 10 μM) for 24 h. Cells were then digested and resuspended in a 1-ml culture medium followed by incubation in the presence of 10 mmol/l rhodamine 123 (Thermo Fisher Scientific, Inc.) for 30 min at 37˚C. After washing three times with PBS, cells were analyzed using a flow cytometer (NovoCyte Advanteon; Agilent Inc.) at an excitation wavelength of 488 nm.

Cell Counting Kit-8 (CCK-8) assay and synergy index assessment. THLE-2, HepG2, Huh7 and Huh1 cells were seeded into a 6-well plate at a density of $1x10^3$ cells/well. Cells were then co-treated with various concentrations of PCA (0, 2.5, 5 and 10 μM) combined with 5-FU (0, 2.5, 5, 10 and 20 μM). Following incubation for 48 h at 37˚C, each well was supplemented with 10 μl CCK-8 reagent (Shanghai Yeasen Biotechnology Co., Ltd.) and cells were cultured for an additional 2 h at 37˚C. The proliferation rate of liver cells was determined by calculating the optical density of each well at a wavelength of 450 nm using the Varioskan LUX multifunctional microplate. The synergistic index of PCA and 5-FU was measured using Compusyn software (version 2.0; ComboSyn, Inc.). A synergistic index of >0.9, 0.9-0.6, 0.6-0.3 and <0.3 indicated no synergy, weak synergy, moderate synergy and strong synergy, respectively.

Cell cycle analysis. HepG2, Huh7 and Huh1 cells were seeded into a 6-well plate at a density of $1x10^5$ cells/well. Subsequently, cells were synchronized for 12 h with DMEM without FBS, followed by treatment with DMSO, PCA (10 μM) or 5-FU (10 μM) and their combination for 48 h. Following digestion, cells were resuspended and fixed in cold 75% ethyl alcohol at 4˚C for 24 h. After washing two times with PBS, cells were stained with propidium iodide (Shanghai Univ Biotechnology Co., Ltd.) for 30 min in the dark at 28˚C. Cell cycle distribution was assessed using a flow cytometer (NovoCyte Advanteon; Agilent Inc.) and analyzed with the FlowJo software (version 7.6.2; FlowJo LLC).

Western blot analysis. Total proteins were extracted from HepG2, Huh7 and Huh1 cells using RIPA reagent supplemented with 1% PMSF (both from Shanghai Univ Biotechnology Co., Ltd.). Following protein quantification using a BCA kit (cat no. abs9232-500T), proteins were separated by 10% SDS-PAGE (Shanghai Univ Biotechnology Co., Ltd.), followed by transferring onto a PVDF membrane (Shanghai Univ Biotechnology Co., Ltd.). Following blocking with 8% skim milk powder in TBS-Tween-20 (0.1%) (TBST) for 2 h at 28˚C, the membranes were incubated with primary antibodies against cyclin-dependent kinase (CDK) 4 (1:2,000; cat no. 11026-1-AP), CDK6 (1:1,000; cat no. 14052-1-AP), ABCG2 (1:1,000; cat no. 27286-1-AP) and GAPDH (1:50,000; cat no. 60004-1-Ig) all from Proteintech Group, Inc. for 16 h at 4˚C. After washing free antibodies three times with TBST, the membranes were incubated for 2 h at 28˚C with the corresponding HRP-conjugated Affinipure Goat Anti-Mouse (1:3,000; cat no. SA00001-1) or HRP-conjugated Affinipure Goat Anti-Rabbit (1:3,000; cat no. SA00001-2) all from Proteintech Group, Inc. secondary antibodies. Finally, the protein bands were visualized using an ECL reagent (Proteintech Group, Inc.), while the expression levels of CDK4, CDK6 and ABCG2 were normalized to those of GAPDH using Image J (version 1.8.0; National Institutes of Health).

Reverse transcription-quantitative (RT-q)PCR experiments. Total RNA was isolated from HepG2, Huh7 and Huh1 cells utilizing TRIzol® reagent (Shanghai Yeasen Biotechnology Co., Ltd.), followed by reverse transcription into cDNA with an mRNA First Strand cDNA Synthesis kit (Takara Bio, Inc.) as per the manufacturer's instructions. Subsequently, quantitative PCR was conducted using the SYBR® Green Master Mix (Takara Bio, Inc.). Following primers were used in the experiments: CDK4 forward, 5'-ATGGCTACCTCT CGATATGAGC-3' and reverse, 5'-CATTGGGGACTCTCA CACTCT-3'; CDK6 forward, 5'-GCTGACCAGCAGTAC GAATG-3' and reverse, 5'-GCACACATCAAACAACCT GACC-3'; and GAPDH forward, 5'-GGAGCGAGATCCCTC CAAAAT-3' and reverse, 5'-GGCTGTTGTCATACTTCT CATGG-3'. Relative mRNA levels of CDK4 and CDK6 were measured using the $2^{-\Delta\Delta Cq}$ method (15), while GAPDH was set as loading control. The qPCR thermocycling protocol consisted of an initial denaturation step at 95˚C for 5 min, followed by 40 cycles of denaturation at 95˚C for 25 sec, annealing at 60˚C for 40 sec and a final elongation step at 72˚C for 30 sec.

Colony formation and 3D sphere formation assays. HepG2, Huh7 and Huh1 cells were plated in a 6-well plate and were then treated with DMSO, PCA (10 μM), 5-FU (10 μM) or their combination for 48 h at 37˚C. For colony formation assays, cells in each group were first digested and were then seeded into a 6-well plate at a density of 500 cells/well. After culturing for 14 days at 37˚C, cell colonies were fixed with 4% paraformaldehyde for 20 min at 28˚C and stained with 1% crystal violet for 30 min at 28˚C (both from Skillbio; Beijing Siqi Biotechnology Co., Ltd.). Following washing with PBS, cell colonies were collected using a vidicon (Sony Group Corporation) while colonies consisting of >50 cells were counted using Image J (version 1.8.0). Furthermore, for 3D sphere formation assay, cells in each group were digested and seeded in a 24-well ultra-low adsorption culture plate (U-section bottom; Absin Biotechnology Co., Ltd.) at a density of 2,000 cells/well. After culturing for 21 days at 37˚C, images of the formed spheres were captured under a light microscope (magnification, x4; Olympus Corporation), while sphere volume was calculated using the following formula: Volume=(length x width^2)/2.

Statistical analysis. All results are presented as the mean ± standard deviation, and all experiments were performed three times. All data were analyzed using SPSS 19.0 software (IBM Corp.). The differences among multiple groups were analyzed by one-way ANOVA followed by Bonferroni's post hoc test. $P<0.05$ was considered to indicate a statistically significant difference.

Results

ABCG2 is a target of PCA. To identify the targets of PCA, the secondary structure of PCA was downloaded from PubChem Compound (Fig. 1A). A total of 55 proteins with binding possibility of ≥0.8 were predicted as targets of PCA using the TargetNet online tool (Fig. 1B). Similarly, a total of 18 proteins with binding possibility of ≥0.8 were predicted as targets of PCA using the Super-PERD database (Fig. 1C). Finally, three proteins, namely ABCG2, GPR35 and TSHR, were intersected in the aforementioned two databases (Fig. 1D). To further analyze the binding capacity between the aforementioned three target proteins and PCA, computer virtual docking was performed using Autodock software. The analysis revealed that ABCG2 displayed the best binding score to PCA (Fig. 1E). The binding score of ABCG2 to PCA was equivalent to that of its positive inhibitor, ML230 (Fig. 1E). In detail, PCA could form five hydrogen bonds with the ASP-128 (2.0 Å), VAL-130 (2.1 Å), GLY-132 (2.5 Å and 2.1 Å), GLY-179 (3.2 Å) and GLN-181 (2.2 Å) sites of ABCG2 (Fig. 1F and G). Overall, the aforementioned findings indicated that ABCG2 could be considered as a key target of PCA.

PCA has high affinity with ABCG2 and inhibits ABCG2 activity in liver cancer cells. To further verify the binding potential between PCA and ABCG2, SPR was carried out. The analysis revealed that the equilibrium dissociation constant (K_d) of PCA to ABCG2 protein was 1.84 μM (Fig. 2A), thus indicating that PCA had high binding affinity to ABCG2. Subsequently, enzyme activity assay was performed and the results revealed that the median effective concentration (EC_{50})

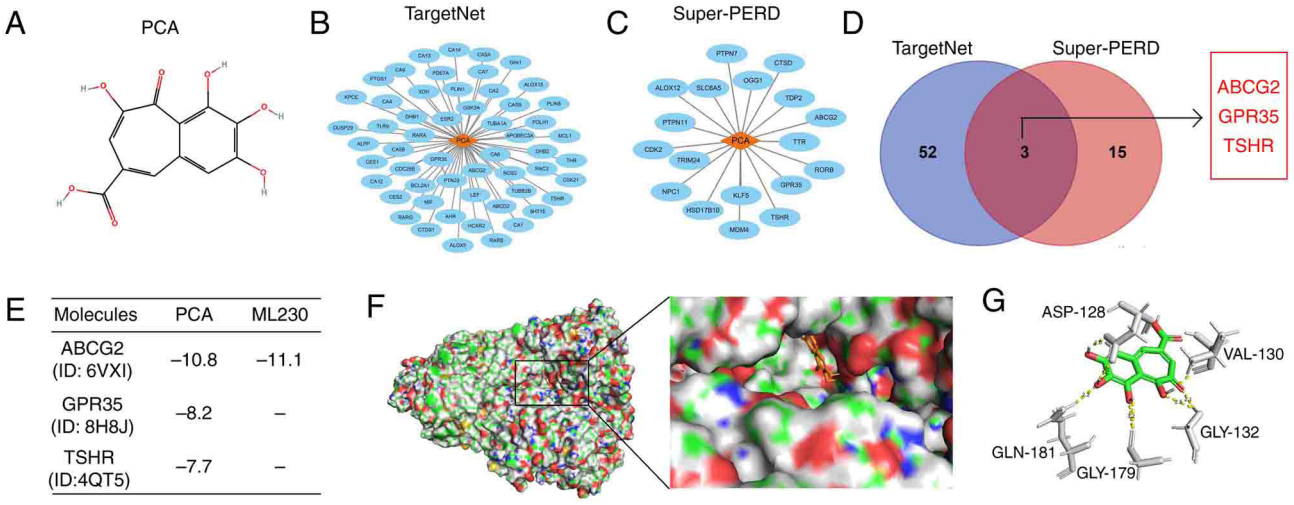

Molecules	PCA	ML230
ABCG2 (ID: 6VXI)	−10.8	−11.1
GPR35 (ID: 8H8J)	−8.2	–
TSHR (ID:4QT5)	−7.7	–

Figure 1. PCA targets ABCG2. (A) The 2D structure of PCA is shown. The protein targets of PCA were predicted using the (B) TargetNet and (C) Super-PERD online tools. (D) The intersected proteins were predicted using both the TargetNet and Super-PERD databases. (E) The computer docking scores of PCA for ABCG2, GPR35 and TSHR are presented. (F and G) Global and local schematic presentation of PCA binding to ABCG2. PCA, purpurogallin carboxylic acid; ABCG2, ATP binding cassette subfamily G member 2; GPR35, G protein-coupled receptor 35; TSHR, thyroid stimulating hormone receptor.

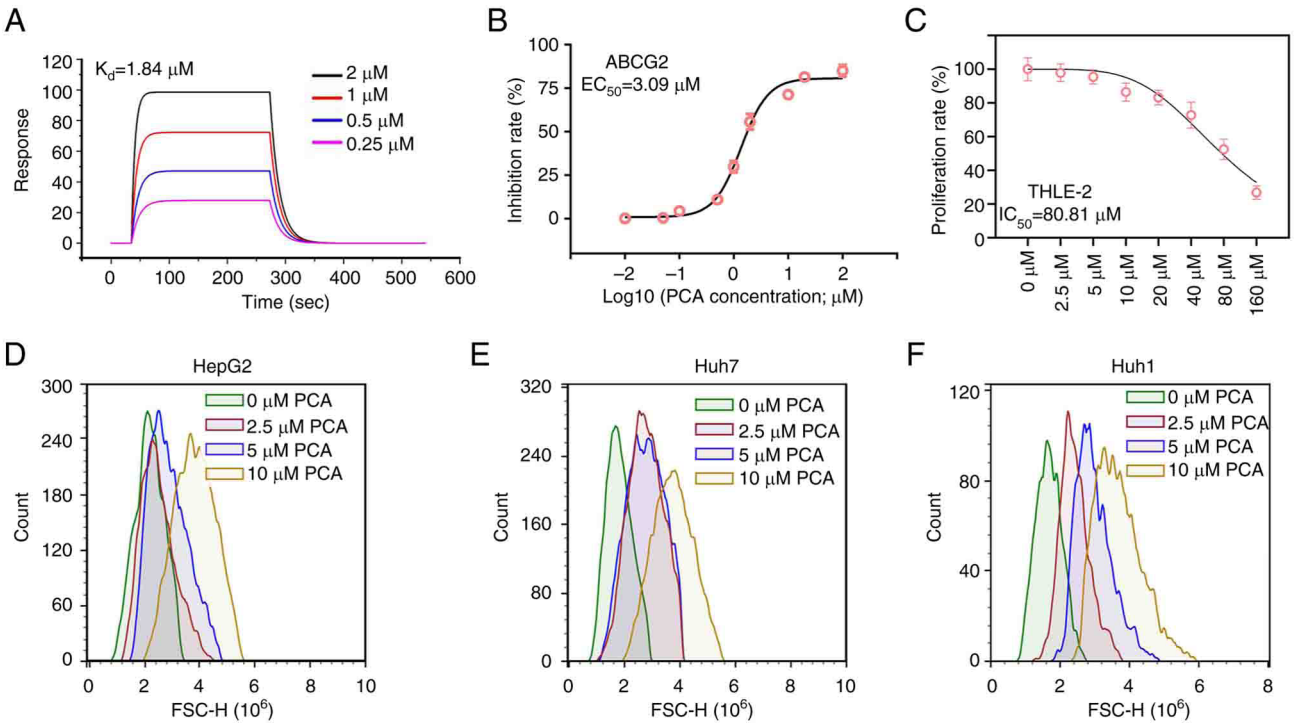

Figure 2. PCA has high affinity for ABCG2 and inhibits its activity in liver cancer cells. (A) Surface plasmon resonance assay was performed to determine the affinity of PCA for ABCG2. (B) The inhibitory effects of PCA on ABCG2 activity are demonstrated. (C) A Cell Counting Kit-8 assay was carried out to measure the non-specific toxicity of PCA on normal THLE-2 hepatocytes. Rhodamine efflux assays were performed to evaluate the drug efflux ability of (D) HepG2, (E) Huh7 and (F) Huh1 cells, following cell treatment with PCA. PCA, purpurogallin carboxylic acid; ABCG2, ATP binding cassette subfamily G member 2.

of PCA for ABCG2 was 3.09 μM (Fig. 2B). Notably, the half-maximal inhibitory concentration (IC_{50}) of PCA in the THLE-2 normal hepatocyte cell line was 80.81 μM (Fig. 2C), thus suggesting that the non-specific toxic effects of PCA on normal cells were low. It has been reported that ABCG2 can efflux drugs from the inside of the cell to the outside. Therefore, rhodamine efflux assays were performed to assess whether PCA could inhibit the efflux capacity of ABCG2. The results demonstrated that PCA could markedly increase the accumulation of rhodamine inside HepG2 (Fig. 2D), Huh7 (Fig. 2E) and Huh1 (Fig. 2F) cells.

PCA exhibits synergistic effects with 5-FU for the inhibition of the proliferation of liver cancer cells. A previous study suggested that targeting ABCG2 could increase the sensitivity of liver cancer cells to chemotherapeutic compounds,

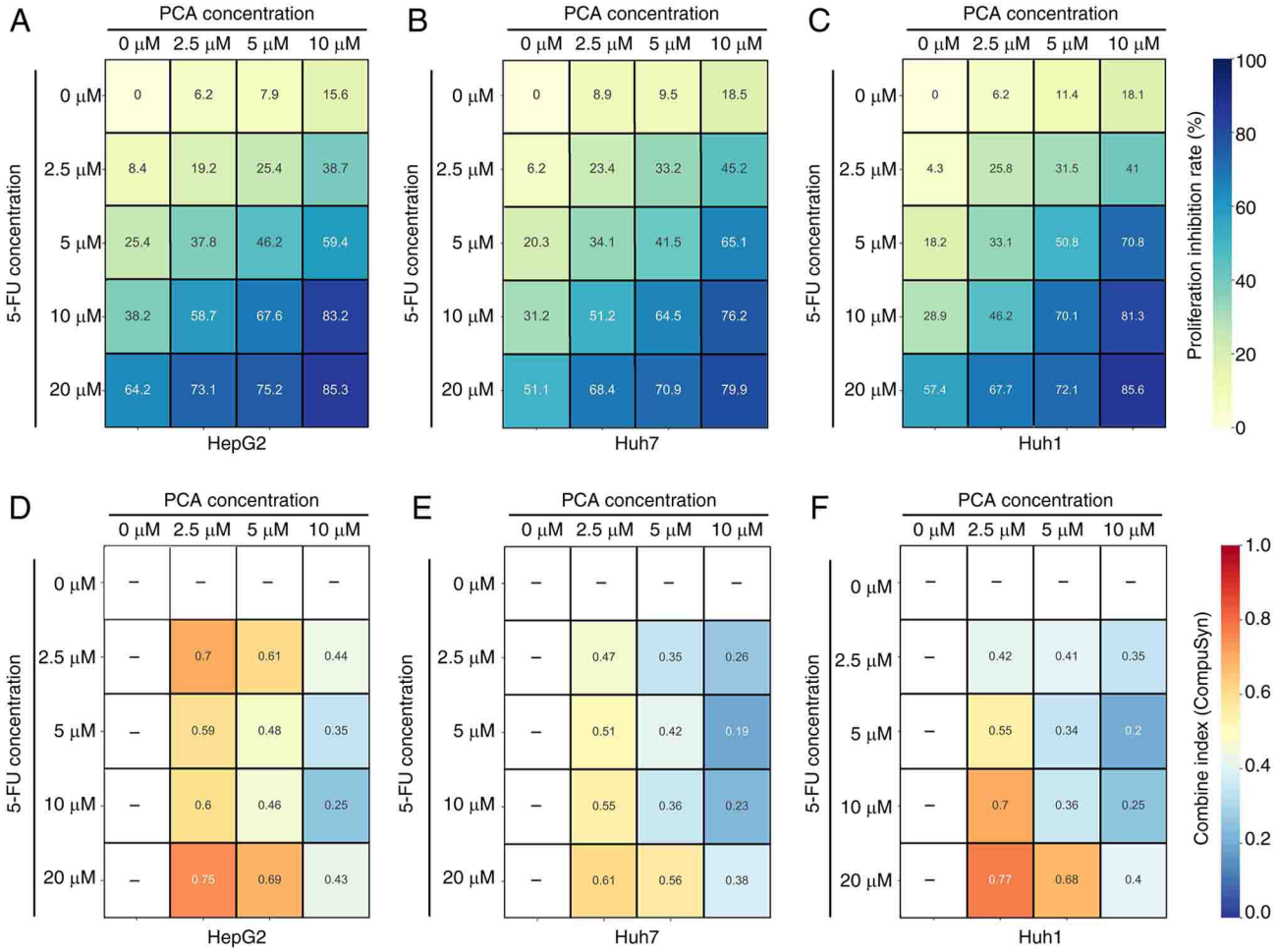

Figure 3. PCA and 5-FU have strong synergistic effects on liver cancer cells. A Cell Counting Kit-8 assay was performed to assess the inhibitory effects of different concentrations of PCA alone or in combination with different concentrations of 5-FU on (A) HepG2, (B) Huh7 and (C) Huh1 cells. Compusyn software was used to evaluate the synergistic effect of different concentrations of PCA combined with 5-FU on (D) HepG2, (E) Huh7 and (F) Huh1 cells. PCA, purpurogallin carboxylic acid; 5-FU, 5-fluorouracil.

including 5-FU (14). Therefore, to assess whether PCA could display synergistic effects with 5-FU, liver cancer cells were treated with various concentrations of PCA (0, 2.5, 5 and 10 μM) combined with 5-FU (0, 2.5, 5 and 10 μM) and then a CCK-8 assay was performed. Detailed proliferation inhibition rates of concentration of each combination (PCA + 5-FU) in HepG2 (Fig. 3A), Huh7 (Fig. 3B) and Huh1 (Fig. 3C) are shown. Based on the inhibition rates, Compusyn software was used to calculate the synergistic index (also named combined index, CI) of each combination. The analysis indicated that 10 μM PCA combined with 10 μM 5-FU had a strong synergistic effect in HepG2 (CI=0.25; Fig. 3D, Huh7 (CI=0.23; Fig. 3E) and Huh1 (CI=0.25; Fig. 3F) cells. Therefore, 10 μM PCA combined with 10 μM 5-FU were considered to present the optimal synergistic profile and these concentrations were therefore used for the subsequent experiments.

PCA exerts synergistic effects with 5-FU on inducing the G_1 phase arrest of liver cancer cells. Cell cycle analysis indicated that 5-FU (10 μM) slightly increased the number of HepG2, Huh7 and Huh1 cells in the G_1 phase of the cell cycle and slightly decreased those in the S phase (Fig. 4A). Additionally, PCA significantly amplified the effects of 5-FU on regulating the cell cycle in liver cancer cells (Fig. 4A). Subsequently, the expression levels of two biomarkers associated with the G_1 phase of the cell cycle, namely CDK4 and CDK6, were detected in liver cancer cells treated with PCA (10 μM), 5-FU (10 μM) or their combination. Therefore, cell treatment with PCA and 5-FU significantly downregulated the protein and mRNA levels of CDK4 and CDK6 in HepG2 (Fig. 4B and E) and Huh7 (Fig. 4C and F) cells. However, the downregulation rate was relatively low. Cell co-treatment with PCA and 5-FU could significantly and acutely reduce the expression levels of both CDK4 and CDK6 in the aforementioned cell lines. In Huh1 cells, cell treatment with PCA or 5-FU alone significantly downregulated the protein and mRNA levels of CDK4, but not those of CDK6 (Fig. 4D and G). Cell co-treatment with both compounds significantly and acutely reduced the expression levels of both CDK4 and CDK6 (Fig. 4D and G). The aforementioned results suggested that PCA could exert a synergistic effect with 5-FU on inducing G_1 phase arrest in liver cancer cells.

PCA has synergistic effects with 5-FU on suppressing the colony and spheroid formation abilities of liver cancer cells. Furthermore, colony formation assays revealed that 5-FU significantly reduced the colony formation ability of liver cancer cells,

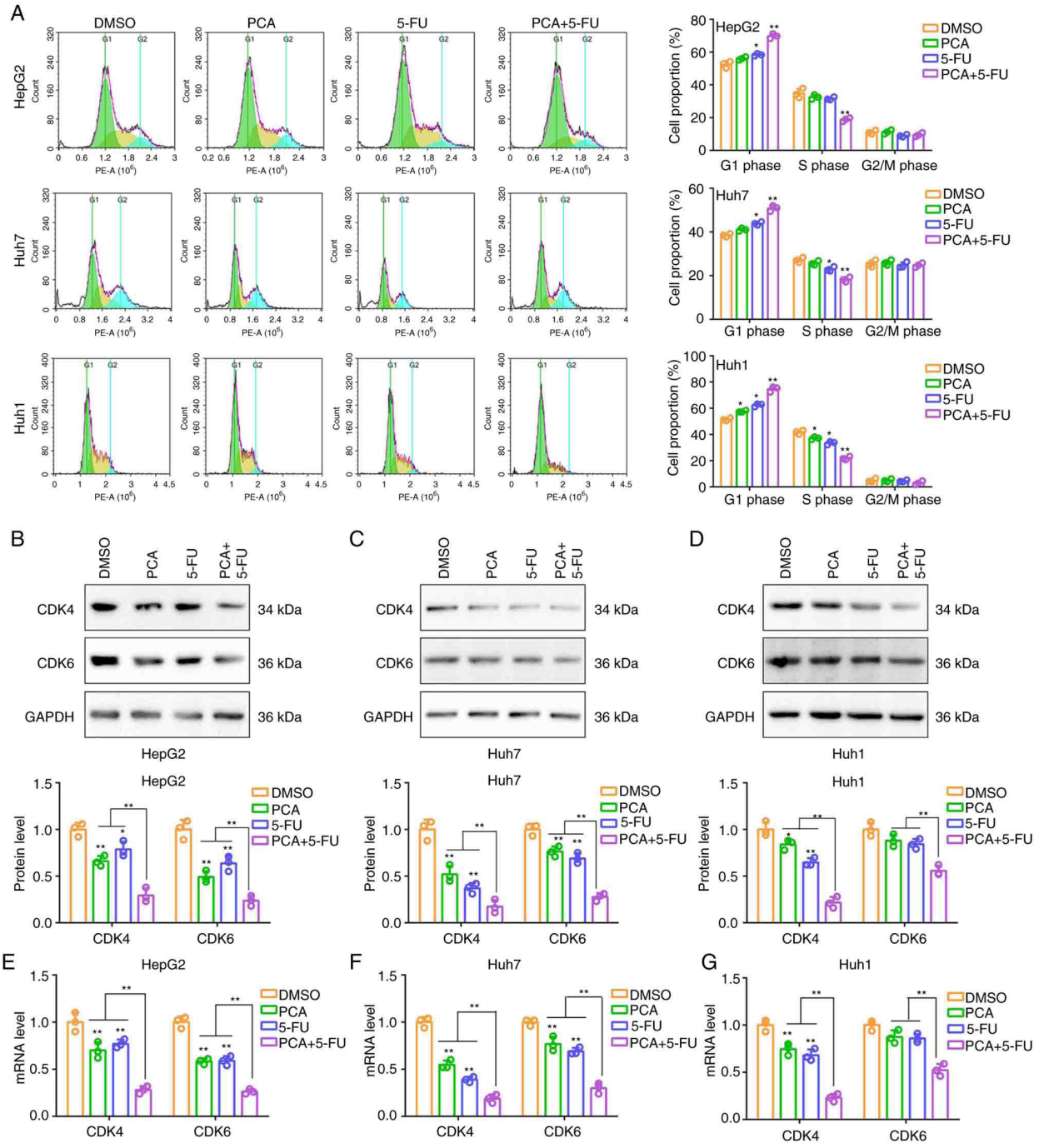

Figure 4. PCA combined with 5-FU induces the G1 phase cell cycle arrest in liver cancer cells. (A) Flow cytometry was carried out to evaluate the cell cycle distribution in HepG2, Huh7 and Huh1 cells treated with DMSO, 10 μM PCA, 10 μM 5-FU or their combination. Western blot analysis was performed to detect the protein expression levels of CDK4 and CDK6 in (B) HepG2, (C) Huh7 and (D) Huh1 cells treated with DMSO, 10 μM PCA, 10 μM 5-FU or their combination. Reverse transcription- quantitative PCR was performed to detect the mRNA levels of CDK4 and CDK6 in (E) HepG2, (F) Huh7 and (G) Huh1 cells treated with DMSO, 10 μM PCA, 10 μM 5-FU or their combination. *P<0.05 and **P<0.01. PCA, purpurogallin carboxylic acid; 5-FU, 5-fluorouracil; CDK, cyclin-dependent kinase.

and PCA significantly amplified the effects of 5-FU (Fig. 5A and B). Additionally, 3D sphere formation assays demonstrated that compared with the number of spheres derived from DMSO-treated cells, that derived for 5-FU-treated cells was slightly lower. However, the number of spheres derived from cells co-treated with 5-FU and PCA was significantly lower (Fig. 5C and D). Taken together, the aforementioned findings indicated that PCA exhibited synergistic effects with 5-FU on attenuating the colony and spheroid formation abilities of liver cancer cells.

PCA has no synergistic effects with 5-FU on inhibiting the proliferation and colony formation abilities of ABCG2-depleted liver cancer cells. To reveal whether the synergistic effects of PCA and 5-FU were dependent on ABCG2, the expression of ABCG2 was silenced in HepG2 and Huh7 cells (Fig. 6A). Therefore, ABCG2 knockdown inhibited the proliferation and colony formation abilities of HepG2 and Huh7 cells (Fig. 6B and C). Cell treatment with 5-FU could further attenuate the proliferation and colony

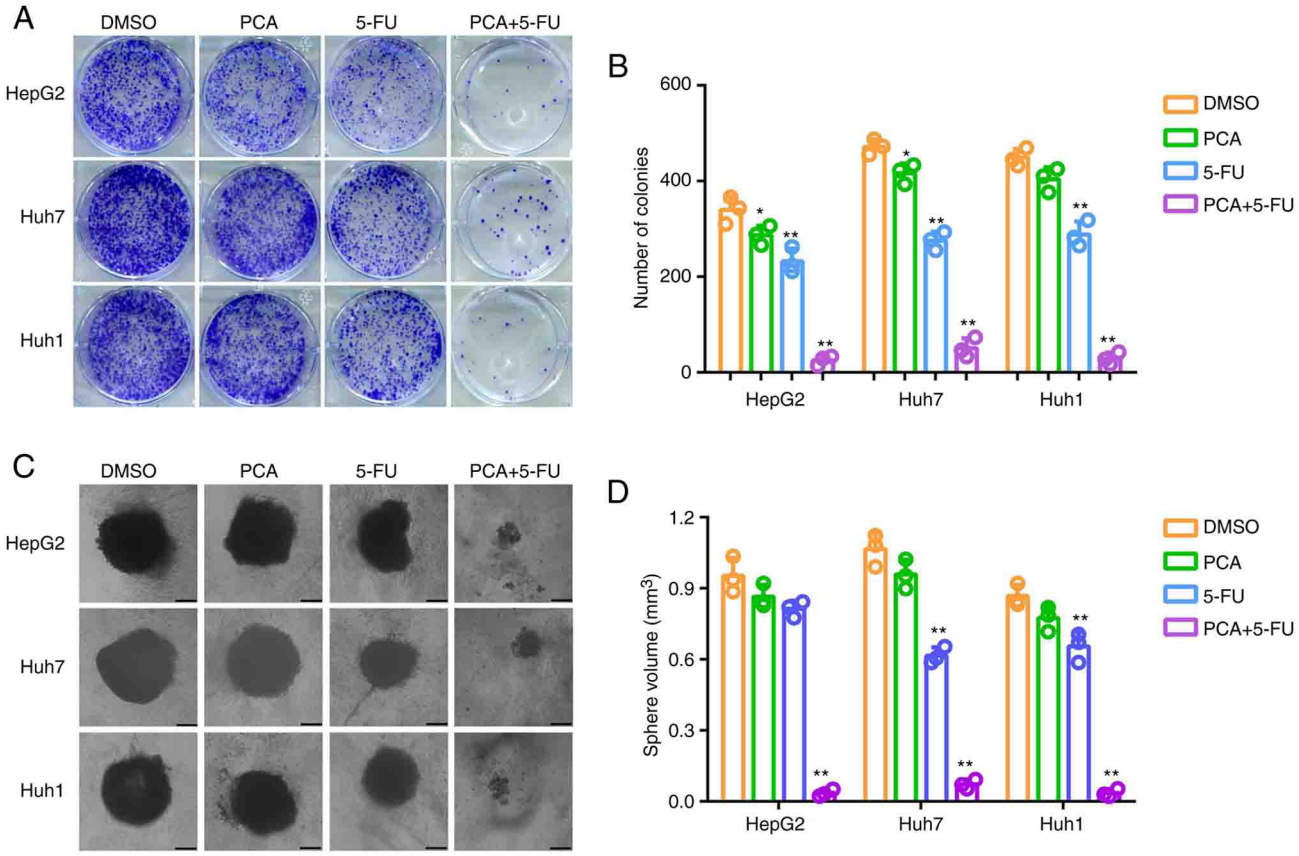

Figure 5. PCA combined with 5-FU suppresses the colony and spheroid formation ability of liver cancer cells. (A and B) Colony formation assays were performed to assess the colony formation ability of HepG2, Huh7 and Huh1 cells treated with DMSO, 10 μM PCA, 10 μM 5-FU or their combination. (C and D) 3D sphere formation assays were carried out to determine the spheroid formation ability of HepG2, Huh7 and Huh1 cells treated with DMSO, 10 μM PCA, 10 μM 5-FU or their combination. *P<0.05 and **P<0.01. PCA, purpurogallin carboxylic acid; 5-FU, 5-fluorouracil.

formation abilities of ABCG2-depleted HepG2 and Huh7 cells (Fig. 6B and C). However, PCA had no effect on inhibiting the aforementioned processes or enhancing the inhibitory effects of 5-FU on ABCG2-depleted HepG2 and Huh7 cells (Fig. 6B and C). The aforementioned findings suggested that the synergistic effects of PCA with 5-FU on liver cancer cells were dependent on ABCG2 expression.

Discussion

5-FU, a nucleoside antimetabolite/analog of uracil, is an effective antitumor drug, which is used to treat liver cancer (16). However, patients with liver cancer are at risk of developing acquired resistance to 5-FU, thus limiting its clinical use (17). It has been reported that p-glycoproteins can promote drug efflux, which is one of the key factors associated with acquired drug resistance (18). Therefore, the development of drugs that target p-glycoproteins could enhance the sensitivity of cancer cells to 5-FU, thus promoting liver cancer therapy.

It has been reported that ABCG2, a member of the p-glycoprotein family, plays a role in the resistance of cancer cells to several therapeutic agents (19). As part of its normal function, ABCG2 transports toxic metabolites from the fetal to the maternal blood vessels of the placenta (20). ABCG2 upregulation in liver cancer tissues was revealed to be associated with poor prognosis and multi-drug resistance (13). Targeting ABCG2 could be a significant strategy to enhance the sensitivity of liver cancer cells to several drugs. A previous study revealed that inhibition of ABCG2 could increase the effects of doxorubicin on eliminating liver cancer stem cells (21). Similarly, ABCG2 knockdown could enhance the sensitivity of liver cancer cells to sorafenib (22). Therefore, the development of drugs targeting ABCG2 could help liver cancer therapy. Actually, several drugs targeting ABCG2 have been reported. For example, isocorydine was demonstrated to suppress ABCG2 activity and induce liver cancer cell apoptosis (23). In addition, chrysin was found to inhibit the expression of ABCG2 and enhance the sensitivity of liver cancer cells to sorafenib (24). However, the majority of the aforementioned natural products exhibited indirect effects on ABCG2. These drugs may mediate some toxic side effects through other targets, while inhibiting the effects of ABCG2.

In the present study, network pharmacology, computer virtual docking and enzymatic activity detection experiments revealed that PCA had high binding affinity to ABCG2 and discriminative activity against ABCG2. Consistently, PCA could significantly inhibit the drug efflux capacity of liver cancer cells. This evidence is consistent with previous theories (25,26) that targeting ABCG2 reduces drug efflux. Actually, in comparison with numerous previously discovered drugs, it is posited that PCA exhibits enhanced specificity for ABCG2 binding, suggesting a potential advantage of PCA.

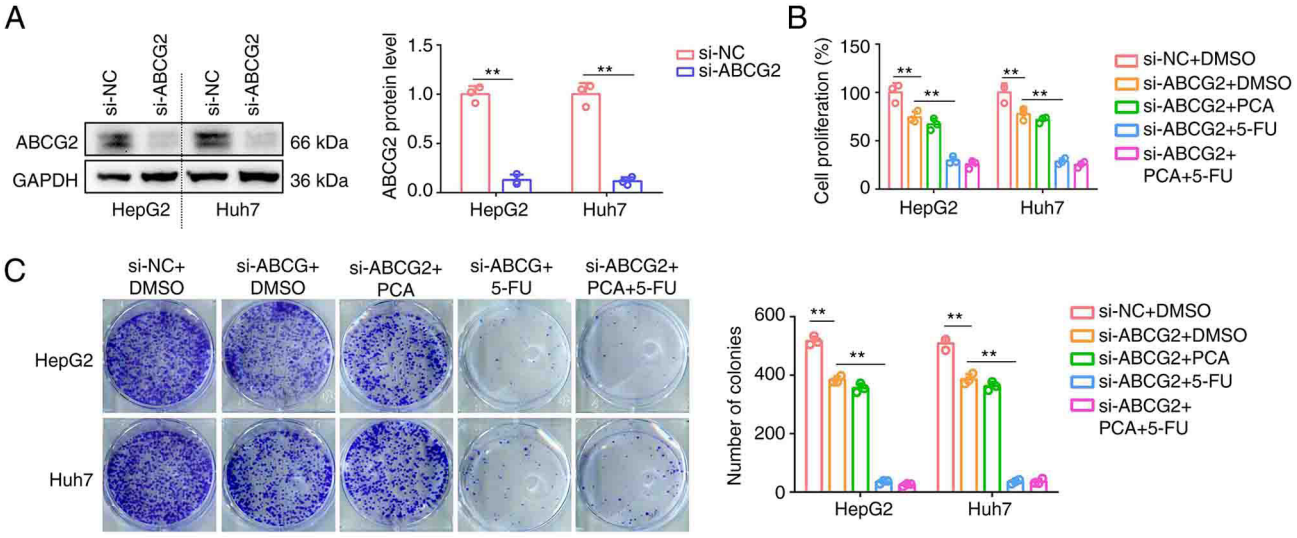

Figure 6. PCA has no synergistic effect with 5-FU on inhibiting the proliferation and colony formation abilities of ABCG2-depleted liver cancer cells. (A) ABCG2-depleted liver cancer cells were established following cell transfection with small interfering RNAs targeting ABCG2. (B) A Cell Counting Kit-8 assay was performed to assess the effects of DMSO, 10 μM PCA, 10 μM 5-FU or their combination on the proliferation ability of ABCG2-depleted HepG2 and Huh7 cells. (C) A colony formation assay was used to evaluate the effects of DMSO, 10 μM PCA, 10 μM 5-FU or their combination on the colony formation ability of ABCG2-depleted HepG2 and Huh7 cells. **P<0.01. PCA, purpurogallin carboxylic acid; 5-FU, 5-fluorouracil; ABCG2, ATP binding cassette subfamily G member 2; si-, small interfering RNA.

Natural products are important molecular libraries for screening the synergistic action of various drugs (27). In fact, the synergistic action between 5-FU and several natural products has been widely reported. Therefore, Zeng *et al* (28) demonstrated that puerarin, a major isoflavone of the kudzu root, displayed synergistic effects with 5-FU in liver cancer cells. Additionally, Li *et al* (29) revealed that tetrandrine derivative could target signal transducer and activator of transcription 3 to enhance the efficacy of 5-FU on targeting liver cancer cells. Furthermore, Cao *et al* (30) suggested that sinomenine combined with 5-FU could synergistically suppress the proliferation of liver cancer cells. However, the aforementioned drug combinations revealed high non-specific toxicity, thus also inhibiting the proliferation of normal cells. Furthermore, low synergy is another issue.

In the present study, the results revealed that PCA, within the pharmacological dose range, exhibited less non-specific toxicity for normal hepatocytes. Further experiments demonstrated that liver cancer cell (HepG2, Huh7 and Huh1) co-treatment with 10 μM PCA and 10 μM 5-FU exhibited a strong synergistic effect on suppressing cell proliferation, and cell colony and spheroid formation, as well as, on inducing G_1 phase arrest. However, the synergistic effect of PCA with 5-FU in liver cancer cells was abrogated following ABCG2 knockdown, thus indicating that the effects of PCA were dependent on ABCG2 expression. This evidence aligned with prior research indicating that targeting ABCG2 can increase the efficacy of chemotherapy drugs. Notably, in comparison with numerous previously discovered drugs, low toxicity is also an advantage of PCA. The present study may provide an effective therapeutic strategy with low toxicity for liver cancer treatment via increasing the sensitivity of cells to 5-FU.

In conclusion, the present study demonstrated that PCA displayed synergistic effects with 5-FU on liver cancer cells *in vitro* via targeting ABCG2. PCA combined with 5-FU could be a potential strategy for liver cancer therapy. However, the present study has some limitations. More importantly, the synergistic effects of PCA and 5-FU on liver cancer was not verified *in vivo*. Therefore, further studies should be performed in the future to confirm the synergistic effect of these two drugs *in vivo*.

Acknowledgements

Not applicable.

Funding

The present study was supported by Task Book of TCM Science and Technology Project in Shandong province (grant no. 2021M089).

Availability of data and materials

The data generated in the present study may be requested from the corresponding author.

Authors' contributions

JL designed the experiments. PZ and WL performed the experiments. SW analyzed the results and wrote the manuscript. All authors read and approved the final version of the manuscript. JL and PZ confirm the authenticity of all the raw data.

Ethics approval and consent to participate

Not applicable.

Patient consent for publication

Not applicable.

Competing interests

The authors declare that they have no competing interests.

References

1. Cao W, Chen HD, Yu YW, Li N and Chen WQ: Changing profiles of cancer burden worldwide and in China: A secondary analysis of the global cancer statistics 2020. Chin Med J (Engl) 134: 783-791, 2021.
2. Chakraborty E and Sarkar D: Emerging therapies for hepatocellular carcinoma (HCC). Cancers (Basel) 14: 2798, 2022.
3. Li QJ, He MK, Chen HW, Fang WQ, Zhou YM, Xu L, Wei W, Zhang YJ, Guo Y, Guo RP, *et al*: Hepatic arterial infusion of oxaliplatin, fluorouracil, and leucovorin versus transarterial chemoembolization for large hepatocellular carcinoma: A randomized phase III trial. J Clin Oncol 40: 150-160, 2022.
4. Ray EM and Sanoff HK: Optimal therapy for patients with hepatocellular carcinoma and resistance or intolerance to sorafenib: Challenges and solutions. J Hepatocell Carcinoma 4: 131-138, 2017.
5. Xu T, Guo P, Pi C, He Y, Yang H, Hou Y, Feng X, Jiang Q, Wei Y and Zhao L: Synergistic Effects of curcumin and 5-fluorouracil on the hepatocellular carcinoma in vivo and vitro through regulating the expression of COX-2 and NF-κB. J Cancer 11: 3955-3964, 2020.
6. Dai W, Gao Q, Qiu J, Yuan J, Wu G and Shen G: Quercetin induces apoptosis and enhances 5-FU therapeutic efficacy in hepatocellular carcinoma. Tumour Biol 37: 6307-6313, 2016.
7. Zeng LH and Wu TW: Purpurogallin is a more powerful protector of kidney cells than trolox and allopurinol. Biochem Cell Biol 70: 684-690, 1992.
8. Zeng LH, Rootman DS, Burnstein A, Wu J and Wu TW: Morin hydrate: A better protector than purpurogallin of corneal endothelial cell damage induced by xanthine oxidase and SIN-1. Curr Eye Res 17: 149-152, 1998.
9. Rambabu M and Jayanthi S: Virtual screening of national cancer institute database for claudin-4 inhibitors: Synthesis, biological evaluation, and molecular dynamics studies. J Cell Biochem 120: 8588-8600, 2019.
10. Mollazadeh S, Sahebkar A, Hadizadeh F, Behravan J and Arabzadeh S: Structural and functional aspects of P-glycoprotein and its inhibitors. Life Sci 214: 118-123, 2018.
11. Kodan A, Futamata R, Kimura Y, Kioka N, Nakatsu T, Kato H and Ueda K: ABCB1/MDR1/P-gp employs an ATP-dependent twist-and-squeeze mechanism to export hydrophobic drugs. FEBS Lett 595: 707-716, 2021.
12. Zattoni IF, Delabio LC, Dutra JP, Kita DH, Scheiffer G, Hembecker M, Pereira GDS, Moure VR and Valdameri G: Targeting breast cancer resistance protein (BCRP/ABCG2): Functional inhibitors and expression modulators. Eur J Med Chem 237: 114346, 2022.
13. Chen YL, Chen PM, Lin PY, Hsiau YT and Chu PY: ABCG2 overexpression confers poor outcomes in hepatocellular carcinoma of elderly patients. Anticancer Res 36: 2983-2988, 2016.
14. Kobayashi K, Higai K, Mukozu T, Matsui D, Amanuma M, Yoshimine N, Ogino Y, Matsui T, Wakui N, Shinohara M, *et al*: Tivantinib decreases hepatocyte growth factor-induced BCRP expression in hepatocellular carcinoma HepG2 cells. Biol Pharm Bull 43: 1421-1425, 2020.
15. Livak KJ and Schmittgen TD: Analysis of relative gene expression data using real-time quantitative PCR and the 2(-Delta Delta C(T)) method. Methods 25: 402-408, 2001.
16. Hou Z, Liu J, Jin Z, Qiu G, Xie Q, Mi S and Huang J: Use of chemotherapy to treat hepatocellular carcinoma. Biosci Trends 16: 31-45, 2022.
17. Li S, Gao M, Li Z, Song L, Gao X, Han J, Wang F, Chen Y, Li W and Yang J: p53 and P-glycoprotein influence chemoresistance in hepatocellular carcinoma. Front Biosci (Elite Ed) 10: 461-468, 2018.
18. Liu X: ABC family transporters. Adv Exp Med Biol 1141: 13-100, 2019.
19. Mao Q and Unadkat JD: Role of the breast cancer resistance protein (BCRP/ABCG2) in drug transport-an update. AAPS J 17: 65-82, 2015.
20. Han LW, Gao C and Mao Q: An update on expression and function of P-gp/ABCB1 and BCRP/ABCG2 in the placenta and fetus. Expert Opin Drug Metab Toxicol 14: 817-829, 2018.
21. Yin W, Xiang D, Wang T, Zhang Y, Pham CV, Zhou S, Jiang G, Hou Y, Zhu Y, Han Y, *et al*: The inhibition of ABCB1/MDR1 or ABCG2/BCRP enables doxorubicin to eliminate liver cancer stem cells. Sci Rep 11: 10791, 2021.
22. Wang M, Wang Z, Zhi X, Ding W, Xiong J, Tao T, Yang Y, Zhang H, Zi X, Zhou W and Huang G: SOX9 enhances sorafenib resistance through upregulating ABCG2 expression in hepatocellular carcinoma. Biomed Pharmacother 129: 110315, 2020.
23. Lu P, Sun H, Zhang L, Hou H, Zhang L, Zhao F, Ge C, Yao M, Wang T and Li J: Isocorydine targets the drug-resistant cellular side population through PDCD4-related apoptosis in hepatocellular carcinoma. Mol Med 18: 1136-1146, 2012.
24. Wei CT, Chen LC, Hsiang YP, Hung YJ, Chien PH, Pan HL and Chen YJ: Chrysin-induced ERK1/2 phosphorylation enhances the sensitivity of human hepatocellular carcinoma cells to sorafenib. Anticancer Res 39: 695-701, 2019.
25. Guo X, To KKW, Chen Z, Wang X, Zhang J, Luo M, Wang F, Yan S and Fu L: Dacomitinib potentiates the efficacy of conventional chemotherapeutic agents via inhibiting the drug efflux function of ABCG2 in vitro and in vivo. J Exp Clin Cancer Res 37: 31, 2018.
26. Bharathiraja P, Yadav P, Sajid A, Ambudkar SV and Prasad NR: Natural medicinal compounds target signal transduction pathways to overcome ABC drug efflux transporter-mediated multidrug resistance in cancer. Drug Resist Updat 71: 101004, 2023.
27. Aung TN, Qu Z, Kortschak RD and Adelson DL: Understanding the effectiveness of natural compound mixtures in cancer through their molecular mode of action. Int J Mol Sci 18: 656, 2017.
28. Zeng YP, Yang ZR, Guo XF, Jun W and Dong WG: Synergistic effect of puerarin and 5-fluorouracil on hepatocellular carcinoma. Oncol Lett 8: 2436-2442, 2014.
29. Li F, Wang J, Wu N, Zhang H, Li Z and Wei N: H1, a derivative of tetrandrine, enhances the efficacy of 5-FU in Bel7402/5-FU cells via suppressing STAT3/MCL-1 and inducing PUMA. Biochem Biophys Res Commun 520: 93-98, 2019.
30. Cao J, Huang J, Gui S and Chu X: Preparation, synergism, and biocompatibility of in situ liquid crystals loaded with sinomenine and 5-fluorouracil for treatment of liver cancer. Int J Nanomedicine 16: 3725-3739, 2021.